ORIGINAL ARTICLE

Observational Study

Simultaneous whole body ¹⁸F-fluorodeoxyglucose positron emission tomography magnetic resonance imaging for evaluation of pediatric cancer: Preliminary experience and comparison with ¹⁸F-fluorodeoxyglucose positron emission tomography computed tomography

Brian S Pugmire, Alexander R Guimaraes, Ruth Lim, Alison M Friedmann, Mary Huang, David Ebb, Howard Weinstein, Onofrio A Catalano, Umar Mahmood, Ciprian Catana, Michael S Gee

Brian S Pugmire, Department of Radiology, Cincinnati Children's Hospital Medical Center, Cincinnati, OH 45229, United States

Alexander R Guimaraes, Division of Body Imaging, Oregon Health Sciences University, Portland, OR 97239, United States

Alexander R Guimaraes, Onofrio A Catalano, Michael S Gee, Division of Abdominal Imaging, Massachusetts General Hospital, Boston, MA 02114, United States

Alexander R Guimaraes, Umar Mahmood, Ciprian Catana, Martinos Center for Biomedical Imaging, Charlestown, MA 02129, United States

Ruth Lim, Umar Mahmood, Division of Nuclear Medicine and Molecular Imaging, Massachusetts General Hospital, Boston, MA 02114, United States

Ruth Lim, Michael S Gee, Division of Pediatric Imaging, MassGeneral Hospital for Children, Boston, MA 02114, United States

Alison M Friedmann, Mary Huang, David Ebb, Howard Weinstein, Division of Pediatric Hematology-Oncology, MassGeneral Hospital for Children, Boston, MA 02114, United States

Correspondence to: Michael S Gee, MD, Division of Pediatric Imaging, MassGeneral Hospital for Children, 55 Fruit St, Boston, MA 02114, United States. msgee@partners.org
Telephone: +1-61-77244207
Fax: +1-61-77268360

Abstract

AIM: To describe our preliminary experience with simultaneous whole body ¹⁸F-fluorodeoxyglucose (¹⁸F-FDG)

positron emission tomography and magnetic resonance imaging (PET-MRI) in the evaluation of pediatric oncology patients.

METHODS: This prospective, observational, single-center study was Health Insurance Portability and Accountability Act-compliant, and institutional review board approved. To be eligible, a patient was required to: (1) have a known or suspected cancer diagnosis; (2) be under the care of a pediatric hematologist/oncologist; and (3) be scheduled for clinically indicated ^{18}F-FDG PET-CT examination at our institution. Patients underwent PET-CT followed by PET-MRI on the same day. PET-CT examinations were performed using standard department protocols. PET-MRI studies were acquired with an integrated 3 Tesla PET-MRI scanner using whole body T1 Dixon, T2 HASTE, EPI diffusion-weighted imaging (DWI) and STIR sequences. No additional radiotracer was given for the PET-MRI examination. Both PET-CT and PET-MRI examinations were reviewed by consensus by two study personnel. Test performance characteristics of PET-MRI, for the detection of malignant lesions, including FDG maximum standardized uptake value (SUVmax) and minimum apparent diffusion coefficient (ADCmin), were calculated on a per lesion basis using PET-CT as a reference standard.

RESULTS: A total of 10 whole body PET-MRI exams were performed in 7 pediatric oncology patients. The mean patient age was 16.1 years (range 12-19 years) including 6 males and 1 female. A total of 20 malignant and 21 benign lesions were identified on PET-CT. PET-MRI SUVmax had excellent correlation with PET-CT SUVmax for both benign and malignant lesions ($R = 0.93$). PET-MRI SUVmax > 2.5 had 100% accuracy for discriminating benign from malignant lesions using PET-computed tomography (CT) reference. Whole body DWI was also evaluated: the mean ADCmin of malignant lesions (780.2 + 326.6) was significantly lower than that of benign lesions (1246.2 + 417.3; $P = 0.0003$; Student's t test). A range of ADCmin thresholds for malignancy were evaluated, from 0.5-1.5×10^{-3} mm^2/s. The 1.0×10^{-3} ADCmin threshold performed best compared with PET-CT reference (68.3% accuracy). However, the accuracy of PET-MRI SUVmax was significantly better than ADCmin for detecting malignant lesions compared with PET-CT reference ($P < 0.0001$; two-tailed McNemar's test).

CONCLUSION: These results suggest a clinical role for simultaneous whole body PET-MRI in evaluating pediatric cancer patients.

Key words: Positron emission tomography; Radiology; Pediatric imaging; Oncology; Cancer; Magnetic resonance imaging

Core tip: Combined positron emission tomography and magnetic resonance imaging (PET-MRI) is an exciting new imaging modality; however, its clinical role remains undefined. PET-MRI has distinct potential advantages for pediatric patients, but the data regarding PET-MRI in children remains limited. We report our experience using PET-MRI in pediatric oncology patients. We found excellent correlation between PET-MRI and PET-computed tomography (CT) maximum standardized uptake values as well as excellent test performance characteristics for PET-MRI using PET-CT as a reference. We also include an evaluation of MRI diffusion weighted imaging in comparison to PET-MRI and PET-CT, which has not been reported previously in the literature.

INTRODUCTION

Combined 18-fluorodeoxyglucose (FDG) positron emission tomography-magnetic resonance imaging (PET-MRI) is a promising new imaging modality. Early results in adult patients have shown that PET-MRI is technically feasible and demonstrates excellent concordance with positron emission tomography-computed tomography (PET-CT) findings[1-9]. PET-MRI has several potential benefits in pediatric cancer patients. First, it holds the promise of improved evaluation of neoplastic disease by combining the superior soft tissue contrast and tissue characterization abilities of MRI, including diffusion-weighted imaging (DWI), with PET metabolic information. This combination is particularly helpful in the evaluation of primary and metastatic malignancies involving the central nervous system, bone marrow, mediastinum, pelvis, and extremities, all of which are relatively common in the pediatric population. Current imaging protocols for these malignancies typically involve separate MRI and PET-CT examinations. The availability of whole body integrated PET-MRI scanners is advantageous both in terms of reducing overall scan times, which would lead to shorter exposure to sedation and anesthesia, as well as improved anatomic registration of PET and MR images due to simultaneous data acquisition[10]. Additionally, by substituting MRI for CT, PET-MRI promises substantially reduced ionizing radiation doses compared to PET-CT. Finally, the superior soft tissue contrast of MRI compared to CT is likely to improve the characterization of incidental indeterminate findings seen on whole body imaging[2], potentially decreasing the need for additional follow-up examinations and/or invasive procedures.

Evidence regarding the performance of integrated

PET-MRI in the pediatric oncology population is relatively sparse compared with adults, with a total of 42 patients included in three published studies[11-13]. The purpose of this study is to evaluate the performance of whole body integrated PET-MRI using ^{18}F-FDG for the detection of malignant lesions in pediatric patients using PET-CT performed earlier on the same day as a reference standard. We compared ^{18}F-FDG standardized uptake values derived from PET-MR with MR-based attenuation correction to those obtained derived from PET-CT with CT attenuation correction. In addition, we evaluated the performance of whole body DWI, which has been shown to be useful for lymphoma staging in both pediatric and adult patients[14,15], for malignant lesion detection compared with PET-CT reference.

MATERIALS AND METHODS

The Institutional Review Board (IRB) of our hospital approved this prospective study, which was Health Insurance Portability and Accountability Act (HIPAA) compliant. Informed consent was obtained from all patients 18 or more years of age and from the parents or legal guardians of all patients under 18 years of age. All patients under the age of the 18 also gave their assent to participation in this study.

Patient selection

In order to be eligible for this study a patient was required to: (1) have a known or suspected cancer diagnosis; (2) be under the care of a pediatric hematologist/oncologist; and (3) be scheduled for clinically indicated ^{18}F-FDG PET-CT examination at our institution. Patients were not eligible to participate if they would require sedation or general anesthesia in order to undergo the PET-MRI examination, were inpatients at the time of their PETCT, had any contraindications to MRI (*e.g.*, non-MRI compatible implants), or were not able to follow directions and hold still for the MRI examination. Patients who underwent additional clinically indicated follow-up PET-CT examinations during the study time period were eligible to undergo an accompanying PET-MRI with each subsequent PET-CT.

Imaging technique

PET-CT: All patients underwent PET-CT examinations prior to PET-MRI, which were performed with a 64-slice PET-CT scanner (Siemens Biograph, Siemens Medical Solutions, Knoxville, TN) on our institution's main hospital campus. While data from the PET-CT were collected for comparison to PET-MRI, the PET-CT was performed based on clinical indications and the decision to obtain the PET-CT scan and the image acquisition protocol of the PET-CT were explicitly not under the control of this study. Therefore, the PET-CT examinations were performed according to standard departmental protocols which include (1) a low-dose attenuation-correction CT (120 kVp, 11 mAs) without intravenous contrast acquired during shallow free breathing from the base of skull to the mid-thigh, followed by (2) PET image acquisition, followed by (3) a diagnostic-quality CT of varying anatomic coverage with or without intravenous contrast (depending on the clinical indication). PET-CT imaging began a mean of 59 min (range 48-78 min) after intravenous FDG administration. PET data underwent automatic attenuation correction using attenuation maps generated from the attenuation-correction CT. The diagnostic CT portion of the examination was performed using standardized, weight-adjusted protocols, including dose modulation, as this is the standard protocol for pediatric patients at our institution.

PET-MRI: Immediately following the PET-CT examinations patients were transported a short distance to an off-campus research facility where the PET-MRI scanner is located. No additional 18-FDG was administered. PET-MRI studies were acquired with a 3 Tesla Biograph mMR scanner (Siemens Medical Solutions, Knoxville, TN) with a 16-channel head and neck surface coil and three or four 12-channel body coils (the number of body coils used was dependent on the height of the patient). These coils were combined to form a multichannel whole-body coil. The PET-MRI acquisitions began a mean of 170 min (range 131-222 min) after FDG injection.

PET acquisition was performed with a 26 cm z-axis field of view and 30% overlap between adjacent table stations. Four to five table positions were acquired based on patient height. The pulse sequences comprising the MRI portion of the PET-MR protocol are summarized in Table 1. MRI acquisitions were simultaneously with PET acquisition starting from the level of the mid-thigh and moving toward the head. Images of the thighs, pelvis, and neck were acquired during shallow free breathing and images of the upper abdomen and thorax were acquired during expiration breath holding. PET data underwent automatic attenuation correction with attenuation maps generated from the two-point Dixon sequence. The FDG administration time was used as the reference time for decay correction. Diffusion weighted imaging was performed using B-values of 50, 400, and 800 s/mm^2.

Statistical analysis

Both PET-CT and PET-MRI examinations were reviewed by consensus by two study personnel (one board certified pediatric radiologist and one radiology resident) using a Syngo workstation (Version 2.00.0000.0014, Siemens Healthcare, Erlangen, Germany). Lesions were identified based on anatomic CT images as abnormally enlarged (> 10 mm diameter) lymph nodes or soft tissue lesions in visceral solid organs or bones. Additional non-enlarged, normal-appearing lymph nodes were included as lesions in the study as control nonmalignant lesions. A maximum standardized uptake value (SUVmax) > 2.5 based on PET-CT imaging was defined as being positive for malignancy. SUVmax values for each lesion on both the PET-CT and PET-MRI were obtained using three-dimensional (3-D) regions of interest (ROIs). The correlation between the SUVmax values obtained

Table 1 Magnetic resonance imaging pulse sequences in pediatric whole body positron emission tomography-magnetic resonance imaging protocol

Pulse sequence	Plane	TR (ms)	TE (ms)	Thk/sp (mm)	Flip angle (°)	BW (Hz/Px)	FOV (cm)	Matrix	TA
T1 Dixon VIBE AC	Coronal	3.6	1.2	3/0	10	965	40-50	192 × 121	0:19
T1 VIBE	Axial	3.9	2.5	3/0	9	720	35-45	288 × 288	0:24
T2 HASTE FS	Axial	1600	95	5/0	9	710	30-40	320 × 260	1:08
EPI DWI	Axial	11000	70	6/0	N/A	2084	30-40	160 × 120	3:51
STIR	Coronal	4000	48	4/0	120	200	35-40	320 × 192	4:54

AC: Attenuation correction; TR: Repetition time; TE: Echo time; BW: Bandwidth; FOV: Field of view; TA: Acquisition time (per table position); VIBE: Volumetric interpolated breath hold examination; HASTE: Half-fourier acquisition single-shot turbo spin echo; FS: Fat suppression; EPI: Echo planar imaging; DWI: Diffusion weighted imaging; STIR: Short tau inversion recovery.

Table 2 Patients and diagnoses

Age at time of diagnosis	Sex	Diagnosis	Total number of PET-MRI examinations
13	Male	Gastrointestinal stromal tumor	3
19	Male	Undifferentiated small round cell sarcoma	1
12	Male	Rhabdomyosarcoma	1
18	Male	Non-Hodgkin's lymphoma (follicular)	1
18	Male	Hodgkin's lymphoma	1
19	Male	Non-Hodgkin's lymphoma (large B-cell)	2
14	Female	Paraganglioma	1

PET-MRI: Positron emission tomography-magnetic resonance imaging.

for each lesion with PET-CT and PET-MR was analyzed using the Pearson correlation coefficient with a statistical significance threshold of $P < 0.05$. Minimum apparent diffusion coefficient (ADCmin) values were also obtained for each lesion based on the lowest value obtained for a voxel on ADC maps within the lesion, and the correlation between the ADCmin and the PET-CT SUVmax values was analyzed using the Pearson correlation method.

Test performance characteristics of PET-MRI, for the detection of malignant lesions, including FDG SUVmax and ADCmin, was calculated on a per lesion basis using PET-CT as a reference standard. Radiation dose estimates for the CT portion of the PET-CT examinations were obtained by converting the dose length product to effective dose (mSv) using standard conversion factors. The effective dose for the PET portion of the PET-CT examinations was calculated using age specific conversion factors previously published by Chawla *et al*[16]. The mean imaging time (total time of image acquisition) was calculated for both PET-CT and PET-MRI and these means were compared using Student's *t*-test.

RESULTS

A total of 10 PET-CT and 10 PET-MRI examinations were performed and evaluated from 7 patients. The mean patient age was 16.1 years (range 12-19 years) including 6 males and 1 female. Their diagnoses included gastrointestinal stromal tumor (GIST), lymphoma (both Hodgkin and non-Hodgkin lymphoma), rhabdomyosarcoma, paraganglioma, and undifferentiated malignant small round cell sarcoma (Table 2), (Figures 1-5). The mean PET-CT image acquisition time was 28.8 min (range 27-31 min) and the mean PET-MRI acquisition time was 75.4 min (range 51-115 min). The mean effective dose imparted by the PET-CT examinations was 12.18 mSv (range 6.1-17.9), whereas the mean effective dose of the PET portion alone was 4.05 mSv (range 3.39-4.9). This difference was statistically significant ($P = 0.004$, Student's *t* test). The mean effective dose for the CT portion of the PET-CT examination was 8.12 mSv (range 2.1-13.0), accounting for 66.7% of the total effective dose for all PET-CT examinations. PET-MRI, by extension, would be associated with an approximately 67% reduction in total effective ionizing radiation dose compared with PET-CT in our pediatric study population.

A total of 20 FDG-avid malignant lesions and 21 non-FDG-avid benign lesions were detected by PET-CT and PET-MRI and included in our analysis. The most common malignant lesion locations were lymph nodes (10), solid abdominal organs (3), lung (3), and bone (2). The correlation between the PET-CT and PET-MRI SUVmax values based on CT attenuation corrected PET-CT and MR attenuation corrected PET-MR imaging was excellent (R = 0.93; $P < 0.0001$) (Figure 6A). Using an SUVmax threshold of > 2.5, PET-MRI SUVmax categorized benign and malignant lesions perfectly compared with PET-CT reference, with an accuracy, sensitivity, and specificity values all of 100% (Table 3). We also evaluated whole-body DWI as an independent biomarker of malignancy compared with PET-CT reference. There was a negative correlation between lesion ADCmin as assessed on DWI and PET-CT SUVmax values, as expected, that was less robust compared with PET-MRI SUVmax (Figure 6B; R = -0.39, $P > 0.05$). The mean ADCmin of malignant lesions (780.2 + 326.6) was significantly lower than that of benign lesions (1246.2 + 417.3; $P = 0.0003$ Student's *t* test). We evaluated the performance of a range of ADCmin thresholds for malignancy, from 0.5-1.5 × 10^{-3} mm²/s. The 1.0 × 10^{-3} ADCmin threshold performed best compared with PET-CT reference (68.3% accuracy; Table 3). However, the accuracy of PET-MRI SUVmax was significantly better than ADCmin for detecting malignant lesions
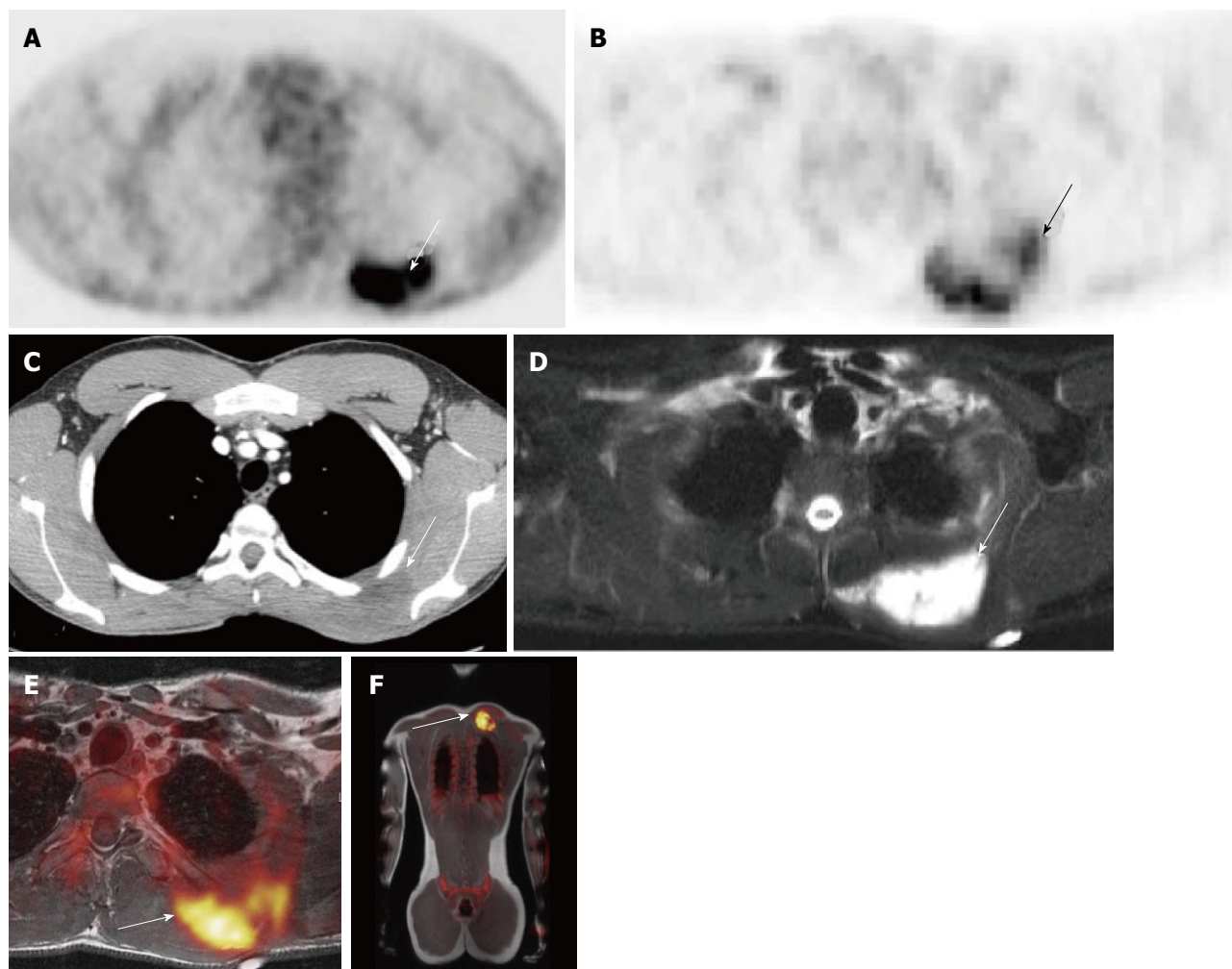
Figure 1 19-year-old male with undifferentiated malignant small round cell sarcoma. Axial image from the PET-CT examination (A) shows intense uptake in mass in the left upper back (white arrow); axial image from the PET-MRI examination (B) shows similar FDG uptake in this region (white arrow); axial CT image from the PET-CT (C) shows a slightly hypodense mass in this region (white arrow). This mass is much better seen on the axial T2 fat suppressed image from the PET-MRI (D) (white arrow). Fused PET-MRI images [T1-weighted axial (E) and whole body coronal (F) MR sequences] again show intense FDG uptake associated with the mass in the left upper back (white arrows). PET-MRI: Positron emission tomography-magnetic resonance imaging; CT: Computed tomography; FDG: Fluorodeoxyglucose.
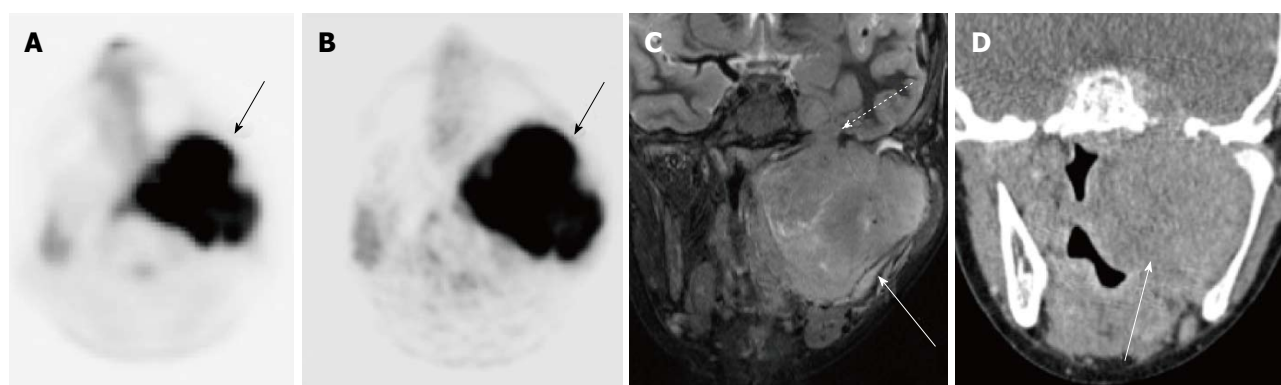
Figure 2 12-year-old male with rhabdomyosarcoma. Axial PET image from PET-MRI (A) shows intense FDG uptake in the left parapharyngeal region (black arrow). Axial PET image from PET-CT (B) shows similar uptake in the same region (black arrow). Coronal T2-weighted fat suppressed image from the MRI portion of the examination (C) clearly shows extent of tumor (white arrow) including perineural spread through foramen rotundum (white dashed arrow). Tumor is not as well delineated on this coronal CT image from the PET-CT examination (D) (white arrow). PET-MRI: Positron emission tomography-magnetic resonance imaging; CT: Computed tomography; FDG: Fluorodeoxyglucose.

compared with PET-CT reference ($P < 0.0001$; two-tailed McNemar's test).
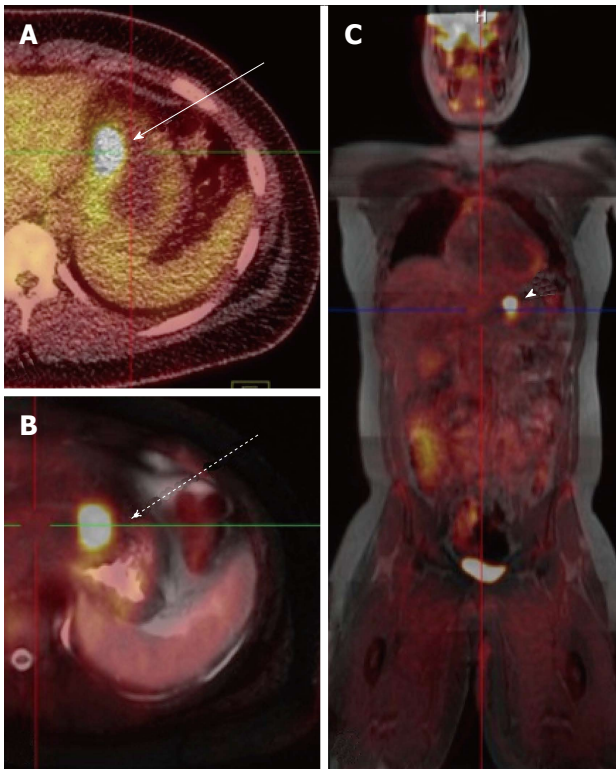
Figure 3 14-year-old male with gastrointestinal stromal tumor. Axial fused PET-CT image (A) shows intense uptake along the lesser curvature of the stomach (white arrow). Axial fused PET-MRI image (B) (T2-weighed HASTE sequence) shows similar intense uptake along the lesser curvature (dashed arrow). Coronal whole body fused PET-MRI image (C) (T1 VIBE sequence) shows intense uptake in the same region (arrowhead). PET-MRI: Positron emission tomography-magnetic resonance imaging; CT: Computed tomography.

DISCUSSION

In this study, we present our initial experience using simultaneous whole body integrated PET-MRI for the evaluation of pediatric oncology patients. Our results demonstrate very good correlation between lesion PET-MRI and PET-CT SUVmax values, which confirms previous results reported by our group and others[7,11,13]. A PET-MRI SUVmax threshold of > 2.5 demonstrated 100% accuracy for detecting malignant lesions seen on PET-CT obtained the same visit. Importantly, PET-MRI was able to accurately detect lesions in both bone and lung, two tissues that can sometimes be associated with segmentation and attenuation correction artifacts on PET-MRI[17,18]. Our results suggest that the Dixon-based MR attenuation correction technique provides accurate whole body tissue attenuation maps across a broad spectrum of tissue types. In addition, the use of 3D ROIs to calculate lesion volumetric SUVmax values may help mitigate small variations in SUV values within a lesion.

We also evaluated the performance of the whole body DWI component of the simultaneous whole body PET-MRI protocol as an independent biomarker of malignancy compared with PET-CT reference. Malignant lesions (defined by PET-CT SUVmax) as a group exhibited a significantly lower ADCmin compared with benign lesions. An ADCmin threshold $< 1.0 \times 10^{-3}$ mm^2/s was the best
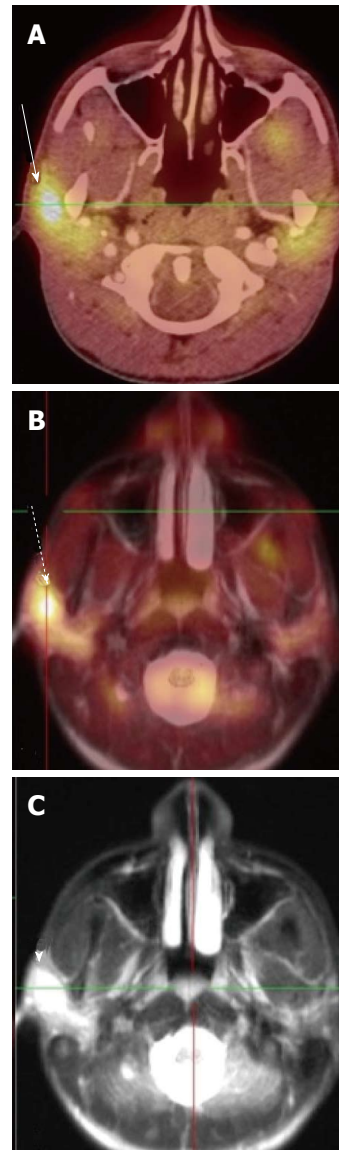

Figure 4 18-year-old male with follicular lymphoma of the right parotid gland. Axial fused PET-CT image (A) shows intense uptake in the region of the right parotid gland (white arrow). Axial fused PET-MRI image (B) (T2 HASTE sequence) shows similar intense uptake in the right parotid (yellow image). Axial T2 HASTE image (C) shows a focal T2-hyperintense mass in the right parotid. This mass was not well seen on CT. PET-MRI: Positron emission tomography-magnetic resonance imaging; CT: Computed tomography.

DWI biomarker of malignancy, with an accuracy of 68.3% and a positive predictive value of 66.7%. Of note, the accuracy of ADCmin was significantly lower than that of PET-MRI SUVmax, suggesting that the PET portion of a combined PET-MRI examination remains a critical component of cancer imaging. Our results are similar to those observed in adult lymphoma patients undergoing PET-MRI[19] and are in keeping with other recent studies suggesting there is no single ADC quantitative threshold that can reliably distinguish benign from malignant lesions in pediatric oncology patients[14,20]. To our knowledge, this is the first study to directly compare DWI ADC and PET-MRI SUV for cancer detection in pediatric patients.

Our results also show that PET-MRI would result in substantial radiation dose savings compared to PET-
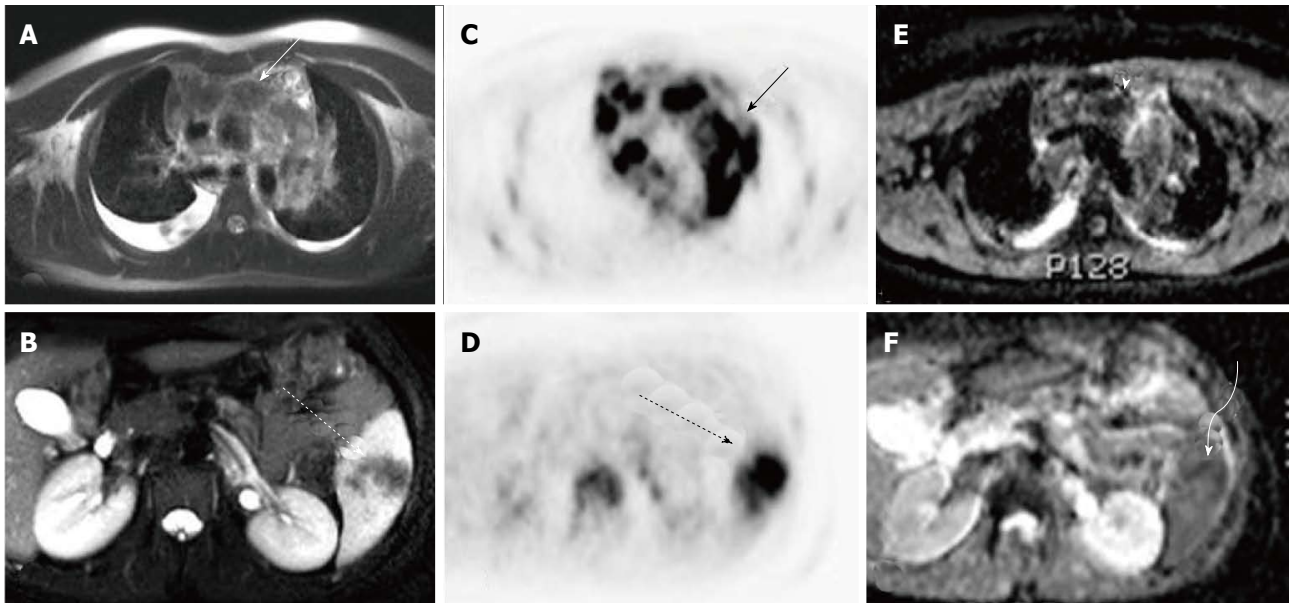
Figure 5 18-year-old male with nodular sclerosing Hodgkin's lymphoma. Axial T2-weighted MRI images of the chest (A) and abdomen (B) demonstrate enlarged mediastinal lymph nodes (white solid arrow) and a region of hypointensity within the spleen (white dashed arrow). Axial images from the concurrently obtained PET examination (C and D) demonstrate intense radiotracer uptake within the mediastinal lymph nodes (solid black arrow) and spleen (dashed black arrow). Axial ADC map images through the same regions (E and F) show areas of decreased signal intensity corresponding to the areas of radiotracer uptake (arrowhead and curve arrow). PET: Positron emission tomography; MRI: Magnetic resonance imaging; ADC: Apparent diffusion coefficient.
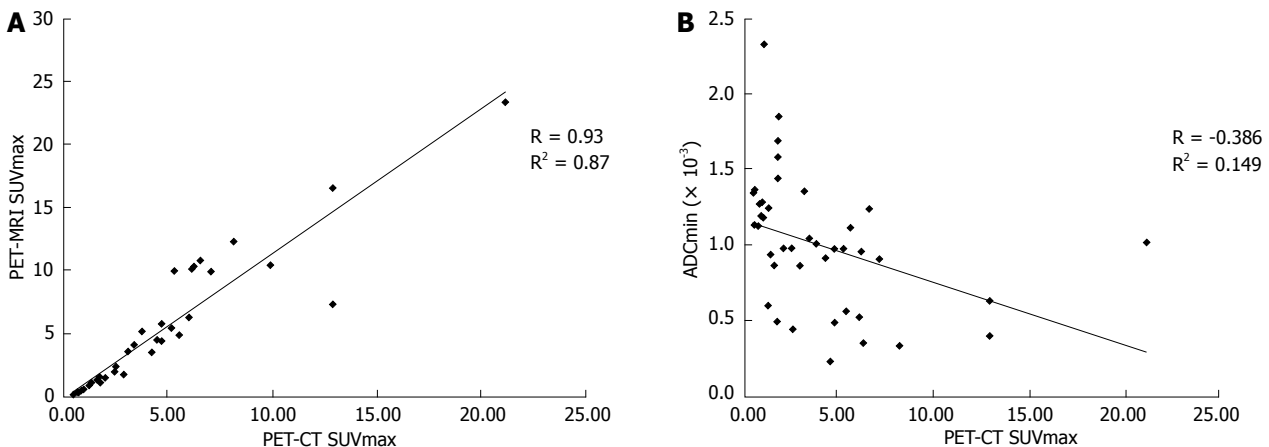
Figure 6 Correlation between positron emission tomography-magnetic resonance imaging biomarkers and positron emission tomography-computed tomography and ADCmin values with positron emission tomography-computed tomography SUVmax. A: PET-MRI SUVmax as a function of PET-CT SUVmax; B: PET-MRI ADCmin as a function of PET-CT SUVmax. PET-MRI: Positron emission tomography-magnetic resonance imaging; CT: Computed tomography; ADCmin: Minimum apparent diffusion coefficient; SUVmax: Maximum standardized uptake value.

CT, with a 67% total reduction in total effective dose. Our results are comparable with those observed in other studies[11-13]. The radiation exposure reduction in this population is predominantly due to the fact that contrast-enhanced diagnostic CT imaging is typically performed as part of the PET-CT exam in the pediatric oncology population at our institution and many others. The substitution of MRI for CT would have a significant impact on radiation reduction in this vulnerable population, especially considering that many of these patients will undergo serial PET-CT imaging for staging and evaluation of treatment response. It should be noted that, while MRI does not use ionizing radiation, it is not without risks, including the theoretical risk of

tissue heating as well as known risks of interactions with implanted material and potential reactions to intravenous contrast material. Additionally, in younger patients MRI frequently requires the use of sedatives or anesthetics, which also carry their own associated risks. PET-CT in very young patients also frequently requires sedation or anesthesia, so the substitution of PET-MRI does not entail an increased risk in this regard.

One issue that may impact routine clinical implementation of PET-MRI is the relatively long scan time compared with PET-CT. However, when considering that many pediatric oncology patients would also routinely require separately-acquired PET-CT and diagnostic MR imaging for local tumor staging, the simultaneous whole

Table 3 Comparative performance of positron emission tomography-magnetic resonance imaging maximum standardized uptake value and minimum apparent diffusion coefficient for lesion detection compared with positron emission tomography-computed tomography reference

Test characteristic	SUVmax > 2.5	ADCmin < 0.5 mm²/s	ADCmin < 1.0 mm²/s	ADCmin < 1.5 mm²/s
Accuracy	100%[1]	61.0%	68.3%	58.5%
Sensitivity	100%	28.6%	70.0%	100.0%
Specificity	100%	95.0%	66.7%	19.0%
Positive predictive value	100%	85.7%	66.7%	54.1%

[1]Indicates statistical significance ($P < 0.001$, two-tailed McNemar's test). ADCmin: Minimum apparent diffusion coefficient; SUVmax: Maximum standardized uptake value.

body PET-MRI acquisition may not increase overall imaging time. The simultaneous whole body PET-MRI acquisition may be an issue for small children who may not be able to tolerate awake scanning without the need for sedation or anesthesia. However, as these children would ordinarily require sedation or anesthesia for PET-CT, PET-MRI would not likely increase their overall exposure to anesthesia related risks. Future research is being directed at developing shorter whole body PET-MRI protocols.

Limitations of our study include the small sample size, relatively older adolescent population, the wide range of tumor types included, and the fact that the research PET-MRI scans were consistently performed after the clinical PET-CT exams. In addition, histologic confirmation was not available for all of the lesions included in the study and we utilized PET-CT as the reference standard. However, all of these patients had histologic confirmation of disease prior to imaging and PET-CT would be considered the imaging standard for detection of malignant lesions in this patient population. Future studies will be needed to evaluate PET-MRI as a sole imaging modality in specific tumor types.

In summary, we present our preliminary results of simultaneous whole body PET-MRI for evaluation of pediatric oncology patients. Our results suggest that PET-MRI has high accuracy for detecting malignant lesions across a wide range of tumor types and anatomic locations, and is associated with a substantial reduction in patient ionizing radiation exposure compared with PET-CT. PET-MRI will likely be increasingly utilized for imaging evaluation of pediatric oncology patients in the near future.

COMMENTS

Background
Positron emission tomography-magnetic resonance imaging (PET-MRI) is a novel imaging technique that combines the spatial and contrast resolution of MRI with the physiologic information provided by PET into one integrated examination. It holds significant promise as a new imaging modality, however the literature regarding this technique in children remains limited.

Research frontiers
While a few early studies have provided preliminary evidence that PET-MRI is

a safe and accurate technique for the evaluation of malignant disease in the pediatric population, further research is needed to confirm these early findings and elucidate the appropriate clinical role for PET-MRI in these patients. Potential areas where PET-MRI may provide added benefit are soft-tissue sarcomas, lymphoma, and brain tumors.

Innovations and breakthroughs
The findings of this prospective observational study confirm the high accuracy of PET-MRI for the detection of malignant lesions, using PET-computed tomography (CT) as a reference. This study is the first to compare PET directly with diffusion weighted imaging in the detection of such lesions and demonstrates the superiority of PET in this application.

Applications
These data provide greater evidence that PET-MRI is an imaging technique which is ready for clinical use as well as more detailed investigation to further define its clinical role.

Terminology
Combined PET-MRI is an imaging technique which allows for the simultaneous acquisition of PET and MRI images. The PET attenuation correction is accomplished through the use of MRI sequences rather than CT images. The PET-MRI images can be fused and viewed simultaneous providing a more complete imaging evaluation of the patient.

Peer-review
This paper describes a research study meant to assess the feasibility and accuracy of PET-MRI in the evaluation of pediatric cancer. The focus of the work is to compare the performance of PET-MRI in its ability, accuracy and utility to detect and characterize cancerous tumors using PET-CT as a reference standard on pediatric oncology patients during the same visit. Obtained results suggest that PET-MRI has high accuracy for detecting malignant lesions across a wide range of tumor types and anatomic locations, and it is associated with a substantial reduction in patient ionizing radiation exposure compared with PET-CT.

REFERENCES

1   **Catalano OA**, Nicolai E, Rosen BR, Luongo A, Catalano M, Iannace C, Guimaraes A, Vangel MG, Mahmood U, Soricelli A, Salvatore M. Comparison of CE-FDG-PET/CT with CE-FDG-PET/MR in the evaluation of osseous metastases in breast cancer patients. *Br J Cancer* 2015; **112**: 1452-1460 [PMID: 25871331 DOI: 10.1038/bjc.2015.112]

2   **Catalano OA**, Rosen BR, Sahani DV, Hahn PF, Guimaraes AR, Vangel MG, Nicolai E, Soricelli A, Salvatore M. Clinical impact of PET/MR imaging in patients with cancer undergoing same-day PET/CT: initial experience in 134 patients--a hypothesis-generating exploratory study. *Radiology* 2013; **269**: 857-869 [PMID: 24009348 DOI: 10.1148/radiol.13131306]

3   **Partovi S**, Robbin MR, Steinbach OC, Kohan A, Rubbert C, Vercher-Conejero JL, Kolthammer JA, Faulhaber P, Paspulati RM, Ros PR. Initial experience of MR/PET in a clinical cancer center. *J Magn Reson Imaging* 2014; **39**: 768-780 [PMID: 24006287 DOI: 10.1002/jmri.24334]

4   **Gaertner FC**, Fürst S, Schwaiger M. PET/MR: a paradigm shift. *Cancer Imaging* 2013; **13**: 36-52 [PMID: 23446110 DOI: 10.1102/1470-7330.2013.0005]

5   **Quick HH**, von Gall C, Zeilinger M, Wiesmüller M, Braun H, Ziegler S, Kuwert T, Uder M, Dörfler A, Kalender WA, Lell M. Integrated whole-body PET/MR hybrid imaging: clinical experience. *Invest Radiol* 2013; **48**: 280-289 [PMID: 23442775 DOI: 10.1097/RLI.0b013e3182845a08]

6   **Schwenzer NF**, Schraml C, Müller M, Brendle C, Sauter A, Spengler W, Pfannenberg AC, Claussen CD, Schmidt H. Pulmonary lesion assessment: comparison of whole-body hybrid MR/PET and PET/CT imaging--pilot study. *Radiology* 2012; **264**: 551-558 [PMID: 22653189 DOI: 10.1148/radiol.12111942]

7   **Drzezga A**, Souvatzoglou M, Eiber M, Beer AJ, Fürst S, Martinez-

Möller A, Nekolla SG, Ziegler S, Ganter C, Rummeny EJ, Schwaiger M. First clinical experience with integrated whole-body PET/MR: comparison to PET/CT in patients with oncologic diagnoses. *J Nucl Med* 2012; **53**: 845-855 [PMID: 22534830 DOI: 10.2967/jnumed.111.098608]

8   **Delso G**, Fürst S, Jakoby B, Ladebeck R, Ganter C, Nekolla SG, Schwaiger M, Ziegler SI. Performance measurements of the Siemens mMR integrated whole-body PET/MR scanner. *J Nucl Med* 2011; **52**: 1914-1922 [PMID: 22080447 DOI: 10.2967/jnumed.111.092726]

9   **Eiber M**, Takei T, Souvatzoglou M, Mayerhoefer ME, Fürst S, Gaertner FC, Loeffelbein DJ, Rummeny EJ, Ziegler SI, Schwaiger M, Beer AJ. Performance of whole-body integrated 18F-FDG PET/MR in comparison to PET/CT for evaluation of malignant bone lesions. *J Nucl Med* 2014; **55**: 191-197 [PMID: 24309383 DOI: 10.2967/jnumed.113.123646]

10 **Rakheja R**, Chandarana H, DeMello L, Jackson K, Geppert C, Faul D, Glielmi C, Friedman KP. Correlation between standardized uptake value and apparent diffusion coefficient of neoplastic lesions evaluated with whole-body simultaneous hybrid PET/MRI. *AJR Am J Roentgenol* 2013; **201**: 1115-1119 [PMID: 24147485 DOI: 10.2214/AJR.13.11304]

11 **Schäfer JF**, Gatidis S, Schmidt H, Gückel B, Bezrukov I, Pfannenberg CA, Reimold M, Ebinger M, Fuchs J, Claussen CD, Schwenzer NF. Simultaneous whole-body PET/MR imaging in comparison to PET/CT in pediatric oncology: initial results. *Radiology* 2014; **273**: 220-231 [PMID: 24877983 DOI: 10.1148/radiol.14131732]

12 **Hirsch FW**, Sattler B, Sorge I, Kurch L, Viehweger A, Ritter L, Werner P, Jochimsen T, Barthel H, Bierbach U, Till H, Sabri O, Kluge R. PET/MR in children. Initial clinical experience in paediatric oncology using an integrated PET/MR scanner. *Pediatr Radiol* 2013; **43**: 860-875 [PMID: 23306377 DOI: 10.1007/s00247-012-2570-4]

13 **Gatidis S**, Schmidt H, Gücke B, Bezrukov I, Seitz G, Ebinger M, Reimold M, Pfannenberg CA, Nikolaou K, Schwenzer NF, Schäfer JF. Comprehensive Oncologic Imaging in Infants and Preschool Children With Substantially Reduced Radiation Exposure Using Combined Simultaneous 18F-Fluorodeoxyglucose Positron Emission Tomography/Magnetic Resonance Imaging: A Direct Comparison to 18F-Fluorodeoxyglucose Positron Emission Tomography/Computed Tomography. *Invest Radiol* 2016; **51**: 7-14 [PMID: 26309185]

14 **Littooij AS**, Kwee TC, Barber I, Granata C, Vermoolen MA, Enríquez G, Zsíros J, Soh SY, de Keizer B, Beek FJ, Hobbelink MG, Bierings MB, Stoker J, Nievelstein RA. Whole-body MRI for initial staging of paediatric lymphoma: prospective comparison to an FDG-PET/CT-based reference standard. *Eur Radiol* 2014; **24**: 1153-1165 [PMID: 24563179 DOI: 10.1007/s00330-014-3114-0]

15 **Siegel MJ**, Jokerst CE, Rajderkar D, Hildebolt CF, Goyal S, Dehdashti F, Wagner Johnston N, Siegel BA. Diffusion-weighted MRI for staging and evaluation of response in diffuse large B-cell lymphoma: a pilot study. *NMR Biomed* 2014; **27**: 681-691 [PMID: 24700565 DOI: 10.1002/nbm.3105]

16 **Chawla SC**, Federman N, Zhang D, Nagata K, Nuthakki S, McNitt-Gray M, Boechat MI. Estimated cumulative radiation dose from PET/CT in children with malignancies: a 5-year retrospective review. *Pediatr Radiol* 2010; **40**: 681-686 [PMID: 19967534 DOI: 10.1007/s00247-009-1434-z]

17 **Attenberger U**, Catana C, Chandarana H, Catalano OA, Friedman K, Schonberg SA, Thrall J, Salvatore M, Rosen BR, Guimaraes AR. Whole-body FDG PET-MR oncologic imaging: pitfalls in clinical interpretation related to inaccurate MR-based attenuation correction. *Abdom Imaging* 2015; **40**: 1374-1386 [PMID: 26025348 DOI: 10.1007/s00261-015-0455-3]

18 **Lyons K**, Seghers V, Williams JL, Sorensen JI, Paldino MJ, Krishnamurthy R, Rohren EM. Qualitative FDG PET Image Assessment Using Automated Three-Segment MR Attenuation Correction Versus CT Attenuation Correction in a Tertiary Pediatric Hospital: A Prospective Study. *AJR Am J Roentgenol* 2015; **205**: 652-658 [PMID: 26295654 DOI: 10.2214/AJR.14.14231]

19 **Heacock L**, Weissbrot J, Raad R, Campbell N, Friedman KP, Ponzo F, Chandarana H. PET/MRI for the evaluation of patients with lymphoma: initial observations. *AJR Am J Roentgenol* 2015; **204**: 842-848 [PMID: 25794075 DOI: 10.2214/AJR.14.13181]

20 **Klenk C**, Gawande R, Uslu L, Khurana A, Qiu D, Quon A, Donig J, Rosenberg J, Luna-Fineman S, Moseley M, Daldrup-Link HE. Ionising radiation-free whole-body MRI versus (18)F-fluorodeoxyglucose PET/CT scans for children and young adults with cancer: a prospective, non-randomised, single-centre study. *Lancet Oncol* 2014; **15**: 275-285 [PMID: 24559803 DOI: 10.1016/S1470-2045(14)70021-X]